

## A Fast Switching Surface Micromachined Electrostatic Relay

Ernst Thielicke, Ernst Obermeier

Microsensor and Actuator Technology (MAT), Berlin University of Technology, Berlin, Germany

Tel.: +49 30 314 72 897, Fax: +49 30 314 72 603, E-mail: oberm@mat.ee.tu-berlin.de

### ABSTRACT

A MEMS relay with electrostatic actuation and novel spring and contact design was developed and tested. This four terminal, single-pole, single-throw normally-open device with bridge contacts (SPST-NO-Bridge) is fabricated by means of a three layer polysilicon surface micromachining process. The total chip-area, including bondpads, is only  $700 \times 700 \mu\text{m}^2$ . Minimum switching voltage is under 30 V and operating voltage is 35 V. High forces along with gold to gold contacts lead to a stable switching behaviour. Contact resistance is  $1.3 \Omega$  (+-10%) and off-resistance is up to  $100 \text{ G}\Omega$ . The microrelay has been tested in ambient air under normal pressure. Results indicate a small change in electrical properties and no change in the mechanical performance when the device is cycled more than  $10^7$  (1 V,  $10 \mu\text{A}$ ) and  $10^4$  (5 V, 1 mA) times. Switching time under normal pressure is below  $100 \mu\text{s}$  (on) and  $50 \mu\text{s}$  (off). This low-power electrostatic relay is very suitable for portable or self-energizing devices, such as Automated Test Equipment (ATE) or reset-switches in charge-amplifiers for piezoelectric sensors.

### INTRODUCTION

Since 1978 [1], micro-relays have been successfully implemented, using different actuation principles and mostly gold-contacts.

Thermomechanical relays [2, 3] generate high forces and large displacements, but their switching time and power consumption is high.

The power consumption in electromagnetic relays [4] is much lower, but the fabrication technology to integrate microcoils and magnetic materials is more complex, and the devices tend to be larger.

Electrostatic microrelays require several orders of magnitude less power than all other actuators. They use the normal force of parallel-plate capacitive actuators and are realized using surface-micromachining with metal [5], polysilicon [6] and SOI [7]. Microrelays with large area actuators made of SOI-material show a very good switching behaviour. However, the application of large SOI-devices is limited by their cost as well as by their size constraints. Furthermore, the switching time is dominated by the squeeze-film-damping effect, which is correlated to the area of the parallel-plates actuator.

Gold and Au-alloys are the materials of choice for micro-contacts. Contact-forces of at least  $100 \mu\text{N}$  lead to contact-resistances around  $1 \Omega$  [8, 9, 10, 11]. The release-forces to reopen the contacts are of the same order of magnitude.

### DEVICE CONCEPT

The actuator is realized by a parallel plate capacitor with circular electrodes. The actuation principle is based on the normal electrostatic force that increases with the inverse square of the electrode-gap. The electrode gap in off-position amounts to  $d = 2 \mu\text{m}$ .

The springs are realized as bending beams with rectangular cross-section ( $b \cdot h$ ). The forces are estimated by the following equations.

$$F_{\text{electrostatic}} = \frac{1}{2} \epsilon_0 U^2 \frac{\pi R^2}{(d-x)^2} \quad F_{\text{spring}} = \frac{Eb h^3}{4l^3} x$$

The electrostatic force is always larger than the spring-forces to keep the actuator moving. With the help of a new spring-design, high contact- and release-forces of up to  $500 \mu\text{N}$  are achieved in a small surface micromachined device. It operates at 20-40 V and the parallel plates come as close as a few hundred nanometers. Figure 1 demonstrates the principle of operation, and Figure 2 shows a SEM-picture of the relay.

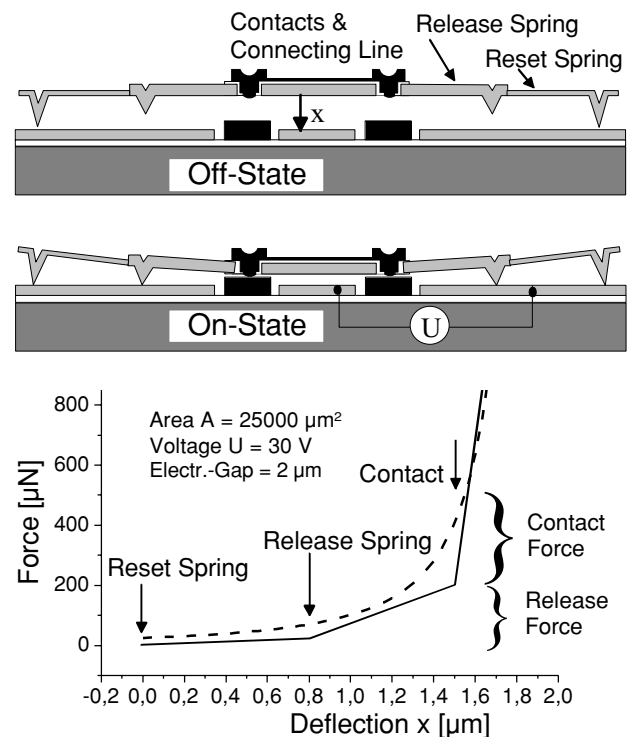


**Figure 1.** Principal operation of the relay actuator with its electrostatic (dotted curve) and spring forces (lines), coupling distances of the springs and contacts (arrows). The plates touch at a deflection of  $2 \mu\text{m}$ .

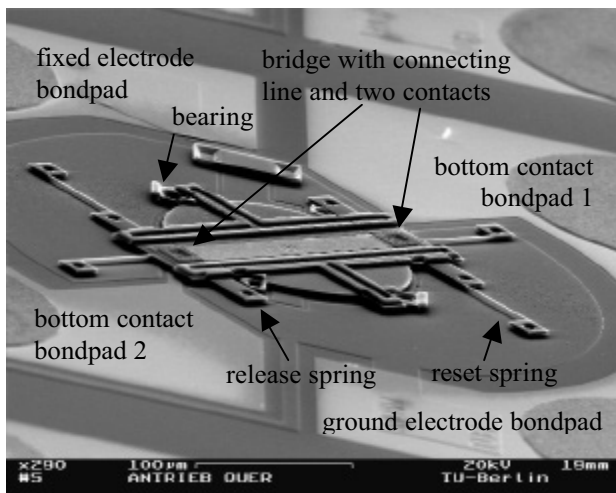


**Figure 2.** SEM-Image of the relay with its armature. Four reset- and four release-springs, the bridge contact and the T-beams are attached to the circular movable electrode to build the armature (cp. Fig. 3). It connects to ground potential via the four reset-springs.

The fixed electrode lies underneath and parallel to the movable electrode. Applying a voltage to the fixed electrode bridges the bottom contacts by moving the armature normal to the wafer surface.

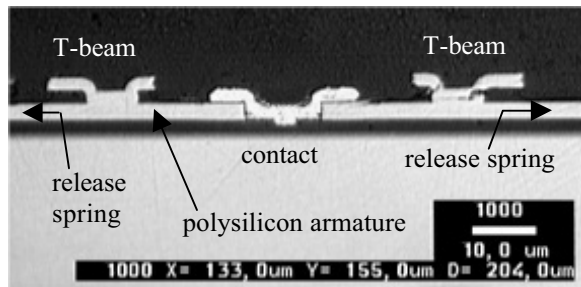


**Figure 3.** Photograph showing the cross-section of the armature with feedthrough contact being part of the bridge. The T-beams run parallel to the connecting line.

The contact-gap in the off-position is wide enough to guarantee a sufficient breakdown voltage. The electrode gap is therefore wide ( $2\ \mu\text{m}$ ), and the electrostatic force in the first part of actuation is small, a reason that the four reset-springs are very soft. These springs allow the armature to move from the off-position to a closer distance of approx.  $1.2\ \mu\text{m}$  ( $= 0.8\ \mu\text{m}$  defl.).

Now, as the electrostatic force increases, four rigid release-springs couple to the substrate and set up the release-force. Contact is made with a deflection of approx.  $1.5\ \mu\text{m}$ . With this deflection, the release spring's deformation is maximum and the required amount of energy for the release actuation is stored.

Now the contact-force increases as long as the bending force of the armature is smaller than the electrostatic force. The armature with T-beams is stiff enough to stop the deflection and prevent a short-circuit of the electrodes (point of intersection in Fig. 1).

This spring design uses the electrostatic force very efficiently and the contact- and release-forces are defined individually by the spring-constants and coupling distances (cp. Fig. 1).

The reset springs connect the armature to ground potential, i.e. the connecting line of the bridge is shielded from the high voltage of the fixed electrode by the movable electrode. There is no interference between control- and load-circuit.

## SIMULATION

The thicknesses of the polysilicon layers are limited, resulting in an armature not as stiff as desired. The armature therefore bends under the electrostatic load. Also, the release springs generate stress in the armature when deflecting.

The behaviour of the relay has been studied using a coupled electrostatic-mechanical FEM-simulation with ANSYS software. For reasons of symmetry, only one quarter of the device is modeled as shown in Figure 4. The reset-springs are ignored, because they do not cause notable stress in the plate.

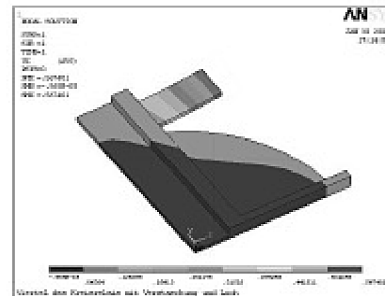


**Figure 4.** FEM-simulated deflection of one quarter of the armature after making contact.

The total electrostatic force is found by integrating over the whole electrode area with the electrode gap varying with the position along the plate. It is maximum when the contacts are closed and the electrode gap is minimum.

The stiffness of small armatures is much higher than that of larger ones. The higher stiffness leads to less deformed electrodes, thus allowing a smaller averaged electrode gap. Smaller devices generate higher forces because the smaller gap more than compensates for the smaller electrode radius.

However, the gap cannot be chosen arbitrarily small, because arcs would short-circuit the electrodes. Taking technological constraints into account, an electrode radius of  $90\ \mu\text{m}$  with a minimum electrode gap of  $300\ \text{nm}$  and an initial contact gap of  $1.5\ \mu\text{m}$  has the best performance. Minimum voltage to close the contacts is  $26\ \text{V}$  and nominal driving voltage for an electrostatic force of  $800\ \mu\text{N}$  is  $35\ \text{V}$ . Short-circuit of the electrodes does not occur before applying more than  $50\ \text{V}$ .

## FABRICATION

The fabrication process uses 16 masks for the patterning of three polysilicon layers, seven sacrificial layers made of LTO, one 160 nm LPCVD-Si<sub>3</sub>N<sub>4</sub>-layer isolating the contacts from the polysilicon-plate and the sputtered and electroplated metallisation.

The ground-electrode and the fixed electrode are made of the first 500 nm thick polysilicon layer. The movable electrode and the springs are made of the second and the T-beams of the third 2.5 μm thick poly-layer. The doped and annealed polysilicon layers are nearly stress free (20 MPa) and have no stress gradients that might bend the armature.

The upper contacts are realized as feedthroughs (12x12 μm<sup>2</sup>) in the poly-Si-armature and their tip is defined by a mould in the sacrificial oxide (cp. Fig. 3). The connecting line and the contact areas are electrically isolated from the armature by a LPCVD-Si-nitride layer. The corresponding process steps are listed in Figure 5, and the contact tip is shown in detail in Figure 6.

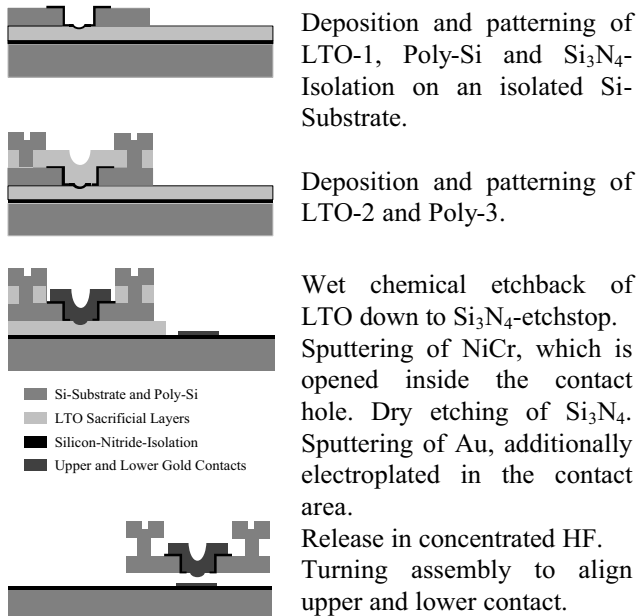


Figure 5. Fabrication steps schematically shown at the cross-section of the contact area (cp. Fig. 3).

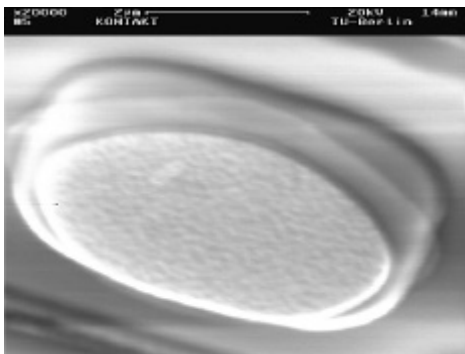


Figure 6. Upper gold contact tip with a diameter of 4 μm.

The coupling distances of the springs and contacts are controlled very precisely by the thicknesses of LPCVD layers and sputtered films. The whole device is built on one substrate without bonding or assembly of chips.

Deposition of polysilicon on metal is not possible, so that the upper and lower contacts are placed next to each other in one fabrication step following the high temperature processes. After releasing the armature, the contacts have to be aligned. For this purpose, four external bearings made of poly-3 hold the armature, which is rotated by 45° using a jet of water or air. Fig. 7 shows the turning motion.

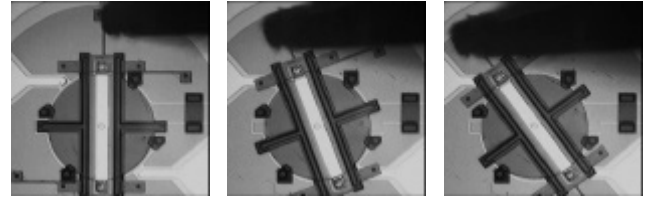


Figure 7. Captured images from a video showing the turning assembly performed by the tip of a microprobe. The relay stays in the turned position and switching direction is normal to the plane of the paper.

## CHARACTERIZATION

The relay has been tested with gold contacts under ambient conditions, and the results are shown in Table 1. The measured breakdown voltage is expected to be higher in dry nitrogen or rare gas.

Table 1. Performance characteristics of the microrelay. Values are for ambient air under normal pressure (10<sup>5</sup> Pa).

Size	350 x 400 μm <sup>2</sup> 700 x 700 μm <sup>2</sup> incl. bondp.
Operation Voltage	35 V
Contact Force (simul.)	250 μN per contact
Release Force (simul.)	150 μN per contact
Contact Resistance	1.3 Ω (+-10%)
Signal Line Resistance	4 Ω
Relay Resistance	6.5 Ω (+-5%)
Off-Resistance	10 <sup>10</sup> Ω @ 100 V 10 <sup>11</sup> Ω @ 20 V
Breakdown Voltage	130 V
Switching Time	100 μs, no bumping
Release Time	50 μs
Load Life	>10 <sup>7</sup> @ 1 V, 10 μA
(pure gold contacts	10 <sup>6</sup> @ 5 V, 100 μA
and resistive load)	10 <sup>4</sup> @ 5 V, 1 mA

Sticking and material transport due to microarcs affect the contact-performance. These effects limit the load life in different ways.

Sticking is a matter of current load and is seen in the testbed when the release time changes from < 100 μs to a much higher value, whereas the effects of microarcs are correlated with the load-inductance and the number of switching cycles.

The microarcs degrade the contacts as shown in Figures 8 to 10. (Resistive load connected with 2 x 1m coaxial cables). Figure 11 shows the contacts after a breakdown at 130 V with current compliance.

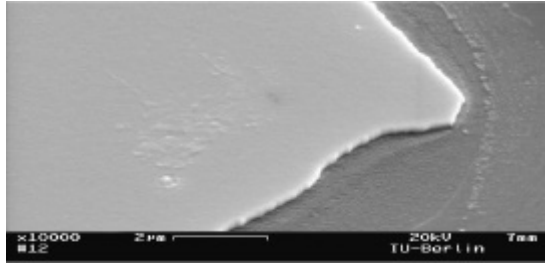


**Figure 8.** Contact switched  $10^7$  times @ 1 V, 10  $\mu$ A. End of lifetime not reached yet.

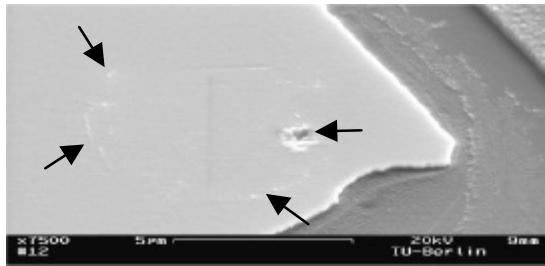


**Figure 9.** Contact switched  $10^4$  times @ 5 V, 1 mA. Microarcs start at the circumference of the upper contact (edges concentrate the electric field, cp. Fig. 6) and cause degradation (see arrows).

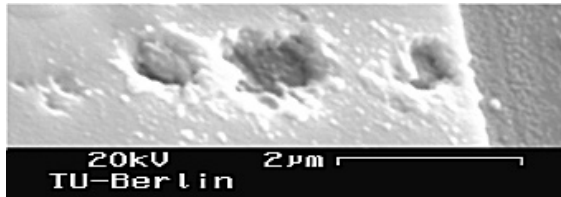


**Figure 10.** Contact switched  $10^6$  times @ 5 V, 100  $\mu$ A. The arcs transport material. Topological change of the contacts and instability in electrical behaviour at the end of the lifetime.

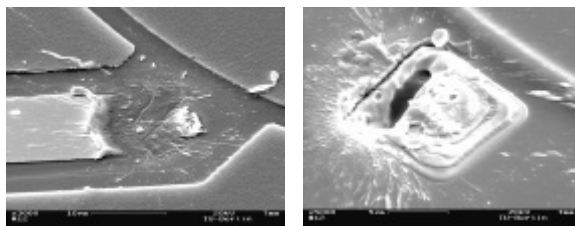


**Figure 11.** Lower (left) and upper (right) contact after destructive breakdown. The contacts are melted partly.

## CONCLUSIONS

The surface micromachined electrostatic relay presented herein combines batch fabrication, small size, low power consumption and stable switching behaviour. It generates higher forces than comparatively small devices in the past and is activated at lower voltages.

The signal line resistance still dominates the relay resistance. It is reduced by a thicker gold layer (actual thickness is 150 nm) and a shorter and wider conductor path to the bondpads. Other contact-materials, such as AuNi, AuCo or Pt might improve the lifetime.

Maximum current carrying capacity is in the region of 20 mA, but then the lifetime is only a couple of cycles. Because the sticking and degradation of microcontacts depends on the load current and load voltage, high lifetimes are easily achieved with small or zero load. Furthermore, loading closed contacts (carry current) is much less challenging than closing and reopening the contacts under the same load. The contact resistance is much lower for higher forces, such as when the contacts are manually closed with a microprobe. In other words, values for lifetime, current carrying capacity and contact resistance can only be compared to values published in the literature, when the test conditions are reported.

The relay is expected to have good properties at high frequencies, because the contact capacitance is low, due to a small contact area, and signal lines can be designed microstrip-compatible.

## References

- [1] K. E. Petersen; Dynamic Micromechanics on Silicon: Techniques and Devices; IEEE Trans. Elec. Dev.; Vol. ED-25; No. 10; 1978
- [2] Cronos, JDS Uniphase, Thermomechanical DC Microrelay, <http://www.memsrus.com/prodrelay.html>
- [3] E. J. J. Kruglick, K. S. J. Pister; MEMS Relay Based Digital Logic Systems; Transducers '99; Sendai; Japan; 818-21
- [4] H. A. C. Tilmans, E. Fullin, H. Ziad, M. D. J. Van de Peer, J. Kesters, E. Van Geffen, J. Bergqvist, M. Pantus, E. Beyne, K. Baert, F. Naso; A Fully-Packaged Electromagnetic Microrelay; Proc. IEEE MEMS Conf. '99
- [5] S. Majumder, N. E. McGruer, P. M. Zavracky, G. G. Adams, R. H. Morrison, J. Krim; Measurement and Modelling of Surface Micromachined, Electrostatically Actuated Microswitches; Transducers '97; Chicago; USA; 1145-8
- [6] M.-A. Gretillat, F. Gretillat, N. F. de Rooij; Micromechanical Relay with Electrostatic Actuation and Metallic Contacts; Transducers '99; Sendai; Japan; 1280-3
- [7] M. Sakata, Y. Komura, T. Seki, K. Kobayashi, K. Sano, S. Horiike; Micro machined Relay which Utilizes Single Crystal Silicon Electrostatic Actuator; Proc. IEEE MEMS Conf. '99
- [8] H. Hosaka, H. Kuwano, K. Yanagisawa; Electromagnetic Microrelays: Concepts and Fundamental Characteristics; Proc. IEEE MEMS Conf. '93
- [9] J. Schimkat; Contact Measurements Providing Basic Design Data for Microrelay Actuators; J. Sen. Act. A; Vol. 73; 1999; 138-43
- [10] D. Hyman, M. Mehregany; Contact Physics of Gold Microcontacts for MEMS Switches; 44<sup>th</sup> Holm IEEE Conf. Elec. Contacts '98; 133-40
- [11] B. L. Pruitt, W.-T. Park, T. W. Kenny; Measurement System for Low Force and Small Displacement Contacts; Sen. Act. Workshop Hilton Head; 2002; Hilton Head; USA